Nucleus accumbens cytoarchitecture predicts weight gain in children

Kristina M. Rapuano[a], Jennifer S. Laurent[b], Donald J. Hagler Jr[c], Sean N. Hatton[d], Wesley K. Thompson[e], Terry L. Jernigan[f,g], Anders M. Dale[c,d], B. J. Casey[a], and Richard Watts[a,1]

[a]Department of Psychology, Yale University, New Haven, CT 06511; [b]College of Nursing and Health Sciences, University of Vermont, Burlington, VT 05405; [c]Department of Radiology, Center for Multimodal Imaging and Genetics, University of California San Diego, La Jolla, CA 92093; [d]Department of Neurosciences, University of California San Diego, La Jolla, CA 92093; [e]Division of Biostatistics, Department of Family Medicine and Public Health, University of California San Diego, La Jolla, CA 92093; [f]Department of Cognitive Science, University of California San Diego, La Jolla, CA 92093; and [g]Center for Human Development, University of California San Diego, La Jolla, CA 92093

The prevalence of obesity in children and adolescents worldwide has quadrupled since 1975 and is a key predictor of obesity later in life. Previous work has consistently observed relationships between macroscale measures of reward-related brain regions (e.g., the nucleus accumbens [NAcc]) and unhealthy eating behaviors and outcomes; however, the mechanisms underlying these associations remain unclear. Recent work has highlighted a potential role of neuroinflammation in the NAcc in animal models of diet-induced obesity. Here, we leverage a diffusion MRI technique, restriction spectrum imaging, to probe the microstructure (cellular density) of subcortical brain regions. More specifically, we test the hypothesis that the cell density of reward-related regions is associated with obesity-related metrics and early weight gain. In a large cohort of nine- and ten-year-olds enrolled in the Adolescent Brain Cognitive Development (ABCD) study, we demonstrate that cellular density in the NAcc is related to individual differences in waist circumference at baseline and is predictive of increases in waist circumference after 1 y. These findings suggest a neurobiological mechanism for pediatric obesity consistent with rodent work showing that high saturated fat diets increase gliosis and neuroinflammation in reward-related brain regions, which in turn lead to further unhealthy eating and obesity.

nucleus accumbens | pediatric obesity | brain development | diffusion MRI | restriction spectrum imaging

The global prevalence of overweight and obesity among youth has risen from 4% in 1975 to over 18% (1) and affects ~35% of children and adolescents within the United States (2). Obesity is associated with negative consequences on an individual's mental health (3–5), physical health (6–8), and on mortality rates (1). Children and adolescents with obesity have more than a fivefold likelihood of becoming obese adults (9) and are likely to have a more substantial obesity-related disease burden (10). Obesity is defined by an excessive amount of fat accumulation and has traditionally been quantified using body mass index (BMI) (11) or BMI scores adjusted for age and sex in children (12). However, BMI differences in thinner individuals are largely attributable to differences in fat-free mass (13), and, conversely, BMI has been suggested to be a poor indicator of severe adiposity (14–16). Recent guidelines have suggested that waist circumference may be a better estimate of visceral adiposity in children within a normal BMI range (e.g., <85% percentile) (17, 18). Consistent with this, waist circumference has been shown to estimate body fat more accurately than BMI (19) and waist-to-hip ratio (WHR) (20). Further, studies have shown waist circumference to outperform BMI in predicting fat gain (21) and obesity-related health risks in children (22, 23), which may be more informative for understanding susceptibility for future health outcomes, such as subclinical inflammation, metabolic dysfunction, and cardiovascular disease (24, 25). Despite the long-term costs and consequences associated with childhood obesity, the neurobiological mechanisms that underlie early weight gain remain unclear.

Previous work has implicated the brain's mesolimbic dopaminergic system—in particular, the nucleus accumbens (NAcc)—in promoting unhealthy eating and other reward-motivated behaviors (26–28). For example, in adults, individual differences in NAcc blood oxygen level-dependent (BOLD) responses to food cues have been positively associated with ad libitum snack consumption (29), weight gain (30), diet failure (31), and BMI (32). Not only have similar associations been observed in children and adolescents (33, 34), but the role of this circuitry may disproportionately affect susceptibility to unhealthy behaviors in youth. Regional and circuit-based changes involving the NAcc appear to precede the maturation of control-related prefrontal circuitry during development (35), which may lead to an overreliance on reward circuitry in driving behavior (36). This imbalance may contribute to and enhance vulnerability for developing unhealthy eating behaviors early in life, thereby increasing risk for obesity during adolescence as well as during adulthood.

Beyond correlational support for associations between obesity-related measures (e.g., BMI, waist circumference) and brain structure and function, a greater understanding of the cytoarchitecture in

Significance

As the prevalence of pediatric obesity continues to rise, determining neurobiological mechanisms underlying longitudinal childhood weight gain is critically important for informing early intervention and prevention strategies. We use an MRI technique to probe nucleus accumbens (NAcc) tissue microstructure and predict waist circumference after 1 y. We find that increased cell density in the NAcc is strongly associated with obesity in a large cohort of children and predicts future weight gain independent of waist circumference at baseline. These results extend animal studies showing a vicious cycle in which diet-induced neuroinflammation leads to disruption of the brain's reward circuitry and subsequently promotes further unhealthy eating and weight gain.

NEUROSCIENCE

key regions within the developing mesolimbic system may yield novel insight into the mechanisms underlying disproportionate weight gain in youth. Recent developments in diffusion magnetic resonance imaging (dMRI) methodology afford the opportunity to probe the tissue microstructure of deep gray nuclei by providing metrics that directly relate to cell and neurite density. Restriction spectrum imaging (RSI) (37, 38) separates the diffusion-weighted MRI signal into distinct components originating in intracellular and extracellular water, which respectively correspond to restricted and hindered diffusion (38) (Fig. 1). This distinction can be used to estimate the degree of cellularity in specific brain structures. For example, a greater proportion of restricted diffusion—along with a parallel decrease in hindered diffusion—is thought to reflect greater tissue cellularity. By approximating the cellular density of specific tissue types, RSI provides an avenue for investigating longitudinal changes in microstructural properties in the developing brain.

Here, we leverage this recent technological advancement to examine the relationship between obesity and subcortical tissue properties in children. More specifically, we evaluated whether NAcc microstructure reflects individual differences in waist circumference in a large cohort of nine- and ten-year-olds ($n > 11,000$) enrolled in the Adolescent Brain Cognitive Development (ABCD) study (39). To further test the possibility that subcortical microstructure is related to early weight gain, we additionally examined whether NAcc cell density at baseline was associated with longitudinal changes in waist circumference after 1 y. We hypothesized that cellularity within the NAcc would not only relate to individual differences in waist circumference but would also prospectively predict increases in waist circumference 1 y later. We provide evidence suggesting that differences in the microstructure of reward-related structures may underlie pediatric obesity and childhood weight gain and propose a potential role of neuroinflammation in mediating the relationship between diet and subsequent weight gain.

Results

A total of 5,790 participants met inclusion criteria (*Methods*) at baseline. Diffusion data passed quality control for 5,366 participants.

Of the 2,212 participants with 1-y follow-up data (ABCD 2.0.1) who met inclusion criteria, diffusion data for 2,133 passed quality control. The demographics of participants included at baseline and year 1 are shown in Table 1.

Baseline Waist Circumference. Mean waist circumference at baseline ($n = 5,366$) was 66.8 cm (SD = 10.4 cm). RSI measures of cellularity within the NAcc were related to waist circumference ($P = 4.3 \times 10^{-58}$; 95% CI: [119, 151 cm]) (Table 2), confirming our a priori hypothesis. More specifically, greater baseline waist circumference was associated with increases in the restricted isotropic component and decreases in the hindered isotropic component within the NAcc ($P = 4.5 \times 10^{-19}$; 95% CI: [−154, −100 cm]) (Table 3). These results remained the same when considering BMI instead of waist circumference (*SI Appendix*, Tables S1 and S2), as well as BMI z-score and BMI percentile (*SI Appendix*, Tables S5 and S6), suggesting that this effect was not specific to either anthropometric measurement. Further, these results were consistent in a uniform subset of participants that were prepubescent (Tanner stage 1) at baseline (*SI Appendix*, Table S3) as well as within a smaller subset of participants that were still prepubescent at follow-up (*SI Appendix*, Table S4).

An exploratory analysis was performed to test for overall associations between cell density in subcortical structures and obesity, correcting for multiple comparisons. Cell density in several subcortical regions was associated with baseline waist circumference in addition to the NAcc (Table 2). All regions demonstrated a significant association between waist circumference and restricted diffusion ($P < 0.05$), but only the caudate ($P = 2.7 \times 10^{-13}$; 95% CI: [−130, −77 cm]), putamen ($P = 1.3 \times 10^{-12}$; 95% CI: [−124, −72 cm]), and pallidum ($P = 3.7 \times 10^{-17}$, 95% CI: [−43, −27]) demonstrated a significant negative association with hindered diffusion. Considering both the increased intracellular (restricted) diffusion and decreased extracellular (hindered) diffusion together, these findings suggest greater cellularity in the caudate, putamen, and pallidum in individuals with greater waist circumference. Despite these significant associations, the NAcc
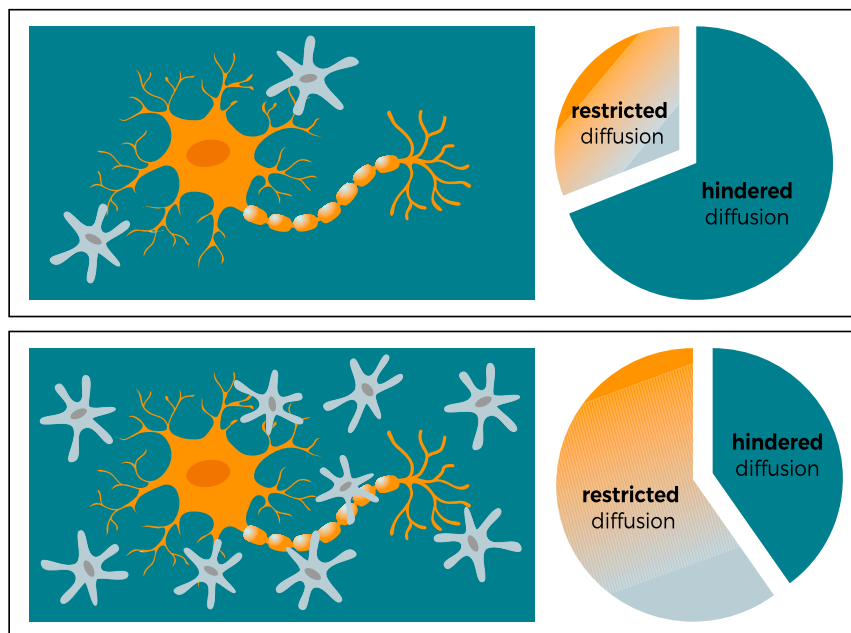
Fig. 1. RSI schematic. Intracellular water diffusion within neurons (orange) and surrounding glial cells (gray) is restricted whereas extracellular water diffusion (teal) is hindered. The proportion of restricted diffusion is inversely related to hindered diffusion whereby greater cell density increases the restricted fraction (*Bottom*) relative to the hindered fraction (*Top*).

Table 1. Subject demographics for analysis of baseline and one-year follow-up

	Baseline	Year 1
n	5,366	2,133
Waist circumference, cm		
Baseline	66.79 ± 10.37	67.01 ± 10.12
Year 1	—	69.76 ± 11.04
BMI, kg/m²		
Baseline	18.47 ± 3.92	18.24 ± 3.62
Year 1	—	19.19 ± 4.13
Interview age, y		
Baseline	9.95 ± 0.62	10.05 ± 0.61
Year 1	—	11.07 ± 0.63
Sex		
Male	2,788 (52.0%)	1,124 (52.7%)
Female	2,578 (48.0%)	1,009 (47.3%)
Race/ethnicity		
White	3,221 (60.0%)	1,438 (67.4%)
Black	685 (12.8%)	179 (8.4%)
Hispanic	919 (17.1%)	329 (15.4%)
Asian	67 (1.2%)	23 (1.1%)
Other	474 (8.8%)	164 (7.7%)
Higher education		
No HS diploma	203 (3.8%)	58 (2.7%)
HS diploma/GED	471 (8.8%)	133 (6.2%)
Some college	1,563 (29.1%)	625 (29.3%)
Bachelor	1,700 (31.7%)	747 (35.0%)
Post graduate degree	1,429 (26.6%)	570 (26.7%)
Household income		
Less than $50,000	1,367 (25.5%)	429 (20.1%)
Between $50,000 and $100,000	1,597 (29.8%)	699 (32.8%)
More than $100,000	2,402 (44.8%)	1,005 (47.1%)
Married		
Yes	3,888 (72.5%)	1,623 (76.1%)
No	1,478 (27.5%)	510 (23.9%)
Baseline ICV, L	1.56 ± 0.14	1.57 ± 0.14

Continuous variables listed as mean ± SD. GED, General Educational Development; HS, high school; ICV, intracranial volume.

remained most strongly associated with waist circumference (Fig. 2) and BMI (*SI Appendix*).

One-Year Change in Waist Circumference. Participants (*n* = 2,133) returned after 1 y for a follow-up visit (mean = 1.03 y, SD = 0.10 y). Mean waist circumference at 1-y follow-up was 69.8 cm (SD = 11.0 cm), and the mean within-subject change was 2.76 cm (SD = 6.33 cm). Change in waist circumference was associated with cell density in the NAcc, such that an increase in waist circumference

was associated with an increase in the restricted component (*P* = 0.001, 95% CI: [16, 52 cm]) and a decrease in the hindered component (*P* = 0.006, 95% CI: [−64, −17 cm]) (Fig. 3). Results were consistent whether or not baseline waist circumference was accounted for in the regression model.

By contrast, an exploratory analysis revealed that no other subcortical regions demonstrated a significant relationship between change in waist circumference and cellularity. Although change in waist circumference was positively associated with the isotropic restricted signal fraction in the caudate and ventral diencephalon (*P* < 0.05) (Table 2), no regions showed a significant decrease in the isotropic hindered signal fraction (Table 3). These findings remained the same when considering BMI instead of waist circumference, such that estimates of increased cellularity within the NAcc—but no other subcortical regions—were significantly associated with increases in BMI after 1 y (*SI Appendix*, Tables S1 and S2) as well as increases in BMI z-score (*SI Appendix*, Table S5) and BMI percentile (*SI Appendix*, Table S6). Results were also consistent within a uniform subset of individuals that were prepubescent at baseline (*SI Appendix*, Table S3) and in individuals that were still prepubescent at follow-up (*SI Appendix*, Table S4).

A post hoc voxelwise analysis of deep gray matter further demonstrated the spatial specificity of our findings. Consistent with the region of interest (ROI) analysis, voxelwise models revealed the most robust relationship between restricted diffusion and change in waist circumference in the NAcc (Fig. 4).

Discussion

The current study observed significant associations between measures of obesity and brain microstructure in a large cohort of 9- and 10-y-old children, particularly within the NAcc. Individual differences in waist circumference were related to RSI estimates of tissue cellularity in several subcortical regions—including the NAcc, caudate, putamen, and pallidum. Among all regions, NAcc cellularity was most strongly related to increases in waist circumference. Moreover, increased waist circumference after 1 y was significantly associated with increased NAcc cell density, such that only this subcortical structure showed both a higher proportion of restricted diffusion and lower proportion of hindered diffusion. Similar effects were observed when evaluating associations with BMI, suggesting that the effects observed in the NAcc were not specific to waist circumference and appear to generalize to other anthropometric measures of obesity. Taken together, these findings provide initial support for a role of microstructural changes in the mechanisms underlying childhood obesity and susceptibility to early weight gain.

One potential explanation for the observed association between waist circumference and NAcc cellularity is that microstructural changes in reward-related regions of the brain are

Table 2. Associations between restricted isotropic component fraction and waist circumference at baseline (*n* = 5,338), and with 1-y change in waist circumference (*n* = 2,121)

	Baseline waist circumference					1-y change in waist circumference				
	Coef	SE	t-value	P value		Coef	SE	t-value	P value	
Thalamus	61.7	9.8	6.29	2.8×10^{-9}	***	19.7	10.1	1.96	0.406	
Caudate	123.8	10.2	12.17	9.9×10^{-33}	***	33.5	10.6	3.15	0.013	*
Putamen	130.8	11.3	11.55	1.4×10^{-29}	***	29.2	12.2	2.38	0.137	
Pallidum	52.1	5.0	10.37	4.8×10^{-24}	***	5.3	5.3	1.00	1.000	
Hippocampus	31.9	10.6	3.01	0.021	*	10.0	10.9	0.92	1.000	
Amygdala	38.8	10.3	3.76	0.001	**	4.6	11.0	0.41	1.000	
Nucleus accumbens	135.3	8.2	16.40	4.3×10^{-58}	***	33.9	9.0	3.77	0.001	**
Ventral diencephalon	82.8	8.9	9.27	2.1×10^{-19}	***	26.3	9.5	2.77	0.046	*

All *P* values Bonferroni corrected for multiple comparisons: *P < 0.05; **P < 0.01; ***P < 1.0 × 10⁻⁶. Coef, coefficient.

NEUROSCIENCE

Table 3. Associations between hindered isotropic component fraction and waist circumference at baseline ($n = 5,338$), and with 1-y change in waist circumference ($n = 2,121$)

	Baseline waist circumference					1-year change in waist circumference				
	Coef	SE	t-value	P value		Coef	SE	t-value	P value	
Thalamus	13.1	7.9	1.65	0.791		−8.3	7.9	−1.06	1.000	
Caudate	−103.9	13.7	−7.60	2.7×10^{-13}	***	−29.3	12.0	−2.45	0.116	
Putamen	−98.8	13.4	−7.39	1.3×10^{-12}	***	−27.6	13.0	−2.11	0.276	
Pallidum	−35.0	4.0	−8.69	3.7×10^{-17}	***	−2.5	4.2	−0.60	1.000	
Hippocampus	7.3	15.1	0.49	1.000		−1.4	13.3	−0.10	1.000	
Amygdala	16.3	20.2	0.80	1.000		9.4	20.5	0.46	1.000	
Nucleus accumbens	−127.1	13.8	−9.19	4.5×10^{-19}	***	−40.5	11.9	−3.39	0.006	**
Ventral diencephalon	−15.8	7.0	−2.26	0.193		−12.6	7.3	−1.73	0.672	

All P values Bonferroni corrected for multiple comparisons: *$P < 0.05$; **$P < 0.01$; ***$P < 1.0 \times 10^{-6}$.

caused by an overconsumption of unhealthy foods. A substantial body of work has documented the role of dopaminergic pathways in motivating eating behavior, which may provide insight into the link between weight change and cellular-level differences in the NAcc. For example, previous studies have demonstrated a decrease in striatal dopamine availability in obese adults (40), suggested to occur as a result of frequent overeating and chronic stimulation. Similar to reward deficiency models of addiction (41), a down-regulation of dopamine may lead individuals to overeat in an attempt to compensate for this deficit. Indeed, decreased mesolimbic dopaminergic activity has been associated with increased consumption of high-fat foods in rodents (42, 43) as well as with emotion-induced eating in humans (44). Consistent with this model, the incentive-sensitization theory of addiction posits that motivational salience, or "wanting," increases disproportionately with food "liking," or the hedonic pleasure associated with consumption—which may even decrease over time (45, 46). Whereas "liking" is considered to primarily depend on the opioid and endocannabinoid systems (47), "wanting" is more closely tied to mesolimbic dopamine pathways (48). Thus, dopaminergic circuitry not only motivates eating behavior but can also be modulated by overconsumption.

Energy consumption also influences physiological signals throughout the brain (49). Homeostatic signals, such as leptin, have been shown to regulate dopaminergic signaling and responses to food cues in the striatum (50, 51). For example, dopamine release in the dorsal striatum is dampened after consumption of a meal (52). In addition to striatal pathways, the ventral pallidum—which has been suggested to play a key role in both the hedonic (53, 54) and motivational aspects of food reward (55, 56)—is sensitive to hypothalamic satiety signaling (57, 58) and physiological states (59). Given the greater cell density of these regions associated with food reward and consumption in children with higher waist circumference, it's interesting to consider the possibility that the microstructural differences observed here are related to diet-induced changes in the developing brain. However, the estimated cellularity of subcortical regions aside from the NAcc were not related to weight gain after 1 y, and thus the directionality of these changes in the brain versus in the body remains an open question.

Under this framework, an excess of highly palatable food consumption may lead to chronic stimulation of regions of the brain associated with food reward and eating behavior and ultimately lead to increased cellularity within these regions. This idea is supported by the current observation that overweight children demonstrated greater cellularity in regions that have been closely associated with various aspects of food reward motivation and eating behavior—including the ventral (NAcc), dorsal striatum (caudate, putamen), and pallidum.

Based on previous work in animal models of diet-induced obesity, an alternative—but complementary—explanation for these

findings may be related to local inflammation of the NAcc. An increase in glial cells (e.g., astrocytes, microglia) can indicate a reaction to circulating proinflammatory signals in the brain (e.g., cytokines) and may also mediate neuroinflammatory responses (60). This process of reactive gliosis has been examined in animal models of obesity by measuring increases in glial fibrillary acidic proteins (GFAPs). For example, there has been substantial evidence demonstrating increased inflammatory markers within the hypothalamus related to diet-induced obesity in rodents (60–64), including changes within hypothalamic glial cells (65, 66) that ultimately interfere with the regulation of food intake (64). Recent work in juvenile rats has extended these findings by demonstrating reactive gliosis within the NAcc induced by a high-calorie diet (67, 68), which has been more specifically linked to the consumption of saturated fats in adult mice (69). Consumption of a diet high in saturated fats not only increased proinflammatory signals in the NAcc but was also associated with compulsive sucrose seeking in mice (69), suggesting that a diet high in saturated fat may trigger neuroinflammation prior to, or independent of, weight gain and may induce high caloric food-seeking behaviors. Thus, diet-induced gliosis implicates a local inflammatory reaction both resulting from and contributing to excess consumption of unhealthy foods, which may explain the observed association between NAcc cellularity and weight gain.

Although animal models provide strong evidence for the presence of gliosis in response to diet-related inflammation, examining this process in vivo has proven to be more challenging in the human brain. Recent efforts to translate animal models of neuroinflammation to noninvasive human neuroimaging have increased (70, 71) but have largely focused on clinical targets using molecular imaging (72). Diffusion RSI analysis (38) provides unique, noninvasive insight into tissue microstructure that
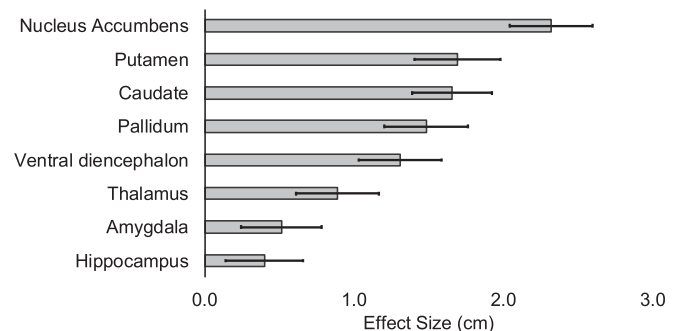
Fig. 2. Association between RSI-based restricted component and baseline waist circumference ($n = 5,214$). Imaging metrics were normalized to have unit SD. Error bars represent 95% CIs.
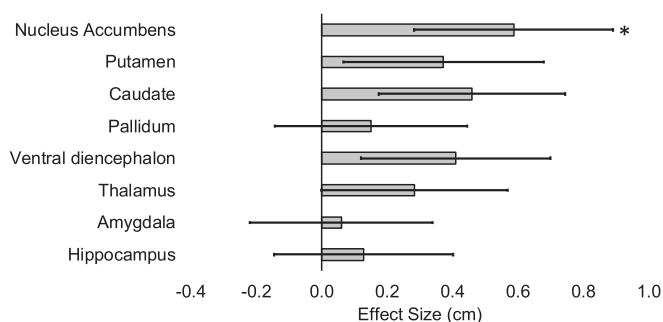
Fig. 3. ROI prediction of 1-y change in waist circumference. Association between RSI-based restricted component and change in waist circumference (accounting for covariates including baseline waist circumference). Imaging metrics were normalized to have unit SD. Error bars represent 95% CIs. Asterisk denotes Bonferroni-corrected significance.

is sensitive to—although not necessarily specific to—cell density and may offer a valuable avenue for future translational studies on neuroinflammation.

A third interpretation based on both human and animal literature is that an unhealthy diet both increases inflammatory signaling as well as decreases dopaminergic signaling and that the combination of these processes contributes to a feed-forward cycle of unhealthy eating and weight gain. Previous work has demonstrated that inflammatory cytokines dampen both striatal dopamine availability (73) and striatal activity during a reward-processing task (74, 75), with respective decreases commensurate with behavioral differences in anhedonia and motivation. Thus, the presence of inflammatory signals in the brain may lead to decreases in dopamine, which may, in turn, perpetuate over-consumption and further inflammation. This cyclical framework is consistent with animal literature demonstrating associations between a high saturated fat diet and decreased dopamine signaling—independent of body weight (43), as well as with reactive gliosis, increased depressive symptoms (akin to anhedonia), and compulsive sucrose seeking (69). The current findings support the possibility that a high saturated fat diet leads to local inflammation of the NAcc and increased glial cell density, which may perpetuate the continued consumption of palatable foods and subsequent weight gain (Fig. 5).

An open question is what factors contribute to the initial consumption that drives subsequent changes in the brain and behavior. Children and adolescents may be at a heightened risk for developing obesity for a variety of reasons. For example, a shift in the balance between developing mesolimbic (e.g., NAcc) and mesocortical circuitry (e.g., prefrontal cortex [PFC]) during adolescence has been suggested to play a role in increasing risk-taking behaviors (76–78), including establishing unhealthy eating habits. Moreover, adolescence is a primary critical period for the development of obesity in childhood (79), in large part due to hormonal changes. In addition, genetics plays a key role in brain development (80) and in determining an individual's striatal dopamine availability (81). One hypothesis suggests that children genetically at risk for obesity show an initial hypersensitivity to palatable food cues which may increase their susceptibility to overeat, and ultimately produce a blunted striatal response by decreasing dopamine signaling (82, 83). This hypothesis is consistent with studies demonstrating heightened striatal sensitivity to food cues in children genetically at-risk for obesity (33), as well as an association between weight gain and blunted striatal responses to food in adults with genetically dampened dopamine signaling (84).

Our findings present a first step toward uncovering the microstructural properties within reward circuitry that promote early weight gain and obesity in children. However, it will be important to consider developmental changes in microstructure as children progress through adolescence. The current analysis provides evidence for predicting longitudinal weight gain based on RSI measurements at baseline, but the extent to which this association changes over the course of development remains an open question. One possibility is that the cellularity of the NAcc measured at specific developmental periods differentially predicts weight gain (e.g., during childhood but not adulthood). In addition to temporal specificity, it will be interesting to assess the spatial specificity of this predictive relationship. The current analysis examined RSI estimates within the subcortex, but further work is needed to assess potential relationships with cortical estimates of RSI across development. Prefrontal cortical (PFC) circuitry develops during adolescence, subsequent to mesostriatal circuitry (76, 77), and plays a key role in controlling reward-related activity and impulsive behavior (78). The developmental shift in the balance between these circuits may parallel the strength of these predictive relationships, such that cellularity in the NAcc—but not the PFC—predicts weight gain during childhood, and PFC cellularity more strongly predicts weight gain during adolescence when imbalances between reward and control circuitry are posited to occur (36). This hypothesis is supported by the notion that we did not find strong evidence of RSI-based cortical associations with waist circumference (*SI Appendix*, Fig. S8). While we did not expect to observe differences in cortical regions associated with cognitive control at this developmental stage, future work will test for differences in both control- and reward-related regions as this cohort ages into adolescence.

Several limitations of the current analysis warrant consideration and provide additional avenues for future work. For example, due to data collection constraints of the ABCD study, the current analysis does not incorporate information regarding dietary intake. Given our hypothesis that a diet high in saturated fat and sugar gives rise to increased neuroinflammation in the NAcc, it is important for future work to explicitly test this hypothesis by considering diet and dietary preferences. The directionality of this
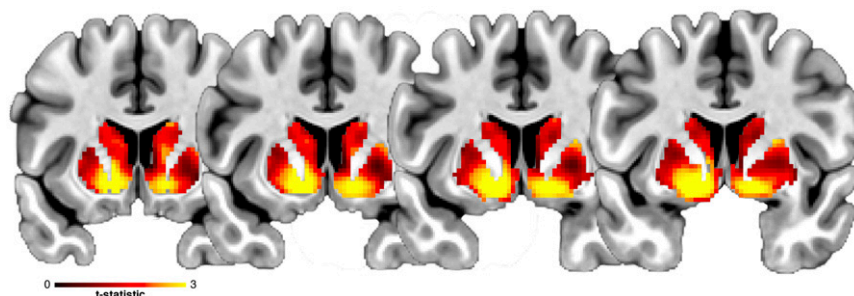
Fig. 4. Voxelwise prediction of 1-y change in waist circumference. Relationship between restricted diffusion fraction and change in waist circumference (accounting for covariates including baseline waist circumference) demonstrates spatial specificity of the ventral striatum.
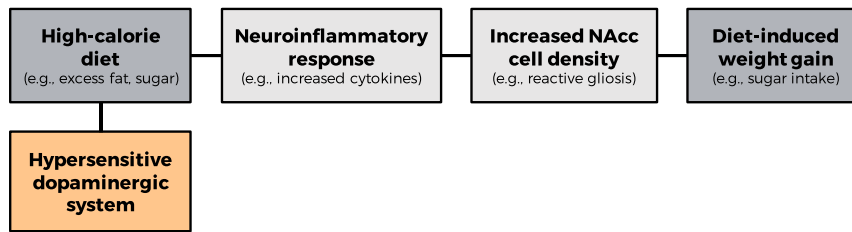
Fig. 5. Proposed mechanism of diet-induced weight gain mediated by NAcc neuroinflammation. The consumption of a high-calorie diet may perpetuate unhealthy eating and subsequent weight gain by promoting inflammatory signaling and corresponding glial proliferation in the NAcc (cf. ref. 68). In this framework, dopaminergic sensitivity early in life may increase susceptibility to unhealthy eating, thereby initiating a cycle of neuroinflammation and continued consumption.

hypothesis will require further work to investigate the underpinnings of the causal relationship between diet, neuroinflammation, and childhood weight gain.

Secondly, the use of waist circumference relative to other anthropometric measurements warrants additional consideration. The current study found a relationship between estimated NAcc cellularity and waist circumference as well as BMI (*SI Appendix*) in children; however, future work will be needed to test the extent to which these relationships generalize across other measures and over the course of development. Whereas waist circumference has been suggested to more effectively measure trunk fat than WHR in youth (20), WHR, but not waist circumference, has been shown to predict mortality in older adults (85). Thus, it is possible that neuroinflammation and associated health risks differentially relate to body shape and fat distribution across the life span.

Future work is needed to examine the role of puberty in the relationship between brain microstructure and weight gain. The current study accounted for pubertal stages measured by self-report, similar to the Tanner scale (86, 87), and further demonstrated sensitivity within uniform subsets of participants that were prepubescent at baseline as well as at the 1-y follow-up (*SI Appendix*, Tables S3 and S4). However, the validity of pubertal self-assessment has previously been challenged (88, 89), particularly within overweight and obese children (90, 91), which may limit the ability of the current analysis to sufficiently control for pubertal stages.

Further, evidence suggests that childhood obesity may lead to earlier puberty (92). Leptin, a hormone that regulates food intake, is produced by adipose tissue and has been shown to be necessary for the onset of puberty (93). Likewise, puberty is associated with a transient increase in insulin resistance (94), which may in turn alter dopaminergic functioning (95). An increase in leptin, combined with a transient increase in insulin resistance has been suggested to be responsible for the earlier onset of puberty in children with higher body fat (96). In addition, leptin plays a role in regulating inflammation in fat cells (97, 98), and this process may be further modulated by dopamine expression (99, 100). Given the complex interactions among dopamine, inflammation, and adipocyte-releasing hormones, future work will be needed to disentangle the contributions of these signals on neuroinflammation within dopaminergic pathways and their role in unhealthy eating and weight gain in children.

We show increased cellularity in the NAcc—a region commonly associated with reward and motivation—in children with greater adiposity, and that this NAcc cellularity predicts weight gain in the same children after 1 y. The current analysis points to the possibility that diet-induced inflammation of the NAcc leads to further unhealthy eating and ultimately weight gain in children. Although many levels of analysis will be needed to unify potential mechanisms underlying obesity and the developing brain, this work begins to integrate findings observed in animal models of obesity with those found in human neuroimaging studies. As an ongoing

longitudinal study, ABCD will provide an opportunity to investigate causal relationships between brain microstructure and weight gain during childhood and adolescence.

Methods

Data Source. The ABCD study is the largest longitudinal study to date dedicated to examining brain development and child health prospectively from 9 y to early adulthood. A large cohort of 9- and 10-y-old children was recruited from 21 sites across the United States, with the goal of enrolling a diverse sample of the US population in regard to race, ethnicity, and socioeconomic status (101). Data are extensively collected using multimodal assessments, including social, behavioral, health, and neuropsychological measures—as well as structural and functional brain imaging—to better understand how social and environmental influences affect brain development, health, emergence of risky behaviors and psychiatric/neurological disorders, and overall life-outcomes trajectory (102). Analyses were conducted on data from the ABCD study 2.0.1 release, which includes baseline data from 11,875 participants and 4,951 participants at a 1-y follow-up (103). Participating study site institutional review boards approved all study procedures. Parents provided written consent, and children provided verbal assent.

Design and Sample. ABCD study recruitment, sample selection, assessments, study design, and data collection are detailed elsewhere (104). Exclusion criteria for the ABCD study included moderate to severe intellectual disability, current substance use disorder, noncorrectable vision, hearing, or sensorimotor impairments, major neurological disorders, gestational age less than 28 wk, birth weight less than 1.2 kg, birth complications requiring more than a 1-mo hospitalization, history of traumatic brain injury, and standard MRI contraindications (e.g., implanted metals, claustrophobia, orthodonture) (104). The current analysis additionally excluded participants with a history of schizophrenia, attention-deficit/hyperactivity disorder (ADHD), autism, neurological disorders (e.g., cerebral palsy, seizures), concussion, diabetes, lead poisoning, muscular dystrophy, multiple sclerosis, or substance abuse. For maximum data consistency, only subjects whose data were acquired using MRI scanners from a single vendor (Siemens Healthineers AG, Erlangen, Germany) were included in our analysis.

Waist circumference was measured by placing a tape measure along the highest point of the pelvic bone. Measurements were collected twice (rounded to the nearest 0.1 inch) and subsequently averaged. Child pubertal status was assessed by self- and parent-report of physical development, yielding a categorical maturation score similar to that of Tanner staging (105).

Image Acquisition. Diffusion images were acquired using a spin echo echo-planar imaging (EPI) acquisition with echo time (TE)/repetition time (TR) = 88/4,100 ms, multiband acceleration factor of 3, phase partial Fourier factor of 0.75, matrix size of 140 × 140, 81 slices, and an axial acquisition with 1.7-mm isotropic resolution. Diffusion weighted data were acquired with six directions at b = 500 s/mm^2, 15 directions at b = 1,000 s/mm^2, 15 directions at b = 2,000 s/mm^2, and 60 directions at b = 3,000 s/mm^2. The full ABCD imaging protocol is described in detail elsewhere (39).

Image Preprocessing. RSI metrics were calculated for subcortical gray matter structures using a linear estimation approach (37, 106, 107). The complete MRI processing pipeline is described in further detail elsewhere (39, 107).

RSI Analyses. All statistical analyses were performed in R Version 3.6.1 (108). Linear mixed effects models (109) were used to evaluate the associations between RSI measures and waist circumference at baseline as well as change in waist circumference at 1-y follow-up. RSI models were generated for each

anatomically defined ROI, including the subcortex. For all models, covariates included fixed effects for sex, interview age, puberty development scale, race/ethnicity, parental education, household income, parents' marital status, and intracranial volume. In addition, the MRI scanner unique identifier and family structure were modeled as nested random effects. The model assessing change in waist circumference was evaluated with and without baseline measurements as a fixed effect covariate in order to isolate unique variance independent of baseline measurements. Significance was assessed using an alpha of 0.05 after Bonferroni correction for multiple comparisons. All effects were consistent bilaterally, and thus RSI measures were averaged between hemispheres for ease of reporting.

In addition to the ROI analyses, a post hoc analysis of voxelwise data was conducted to further evaluate the spatial specificity of our findings. The same model used for the ROI analyses was applied to every voxel contained within the same subcortical mask (R Version 3.6.1) (108). Relationships with RSI measures were tested for baseline waist circumference as well as for 1-y change in waist circumference.

Subcortical RSI estimates were also compared to BMI at baseline and at 1-y follow-up given the ubiquity of this measure in the literature. These analyses were performed using identical predictors and covariates as in the models evaluating waist circumference. To demonstrate consistency across related measures, relationships with BMI percentile (adjusted for age and sex) and BMI z-scores were also assessed. The 2000 CDC growth charts were used to compute adjusted measurements in SAS (110).

Code Availability. All code for data extraction and analysis used in this study will be made available for download from https://github.com/ABCD-STUDY.

1. World Health Organization, Obesity and overweight. https://www.who.int/news-room/fact-sheets/detail/obesity-and-overweight. Accessed 24 September 2020.
2. C. D. Fryar, M. D. Carroll, C. L. Ogden, "Prevalence of overweight, obesity, and severe obesity among children and adolescents aged 2–19 years: United States, 1963–1965 through 2015–2016" (National Center for Health Statistics Health E-Stat, 2018).
3. J. Wardle, L. Cooke, The impact of obesity on psychological well-being. *Best Pract. Res. Clin. Endocrinol. Metab.* **19**, 421–440 (2005).
4. R. M. Puhl, J. D. Latner, Stigma, obesity, and the health of the nation's children. *Psychol. Bull.* **133**, 557–580 (2007).
5. J. J. Puder, S. Munsch, Psychological correlates of childhood obesity. *Int. J. Obes.* **34** (suppl. 2), S37–S43 (2010).
6. A. T. Cote, K. C. Harris, C. Panagiotopoulos, G. G. S. Sandor, A. M. Devlin, Childhood obesity and cardiovascular dysfunction. *J. Am. Coll. Cardiol.* **62**, 1309–1319 (2013).
7. L. J. Lloyd, S. C. Langley-Evans, S. McMullen, Childhood obesity and risk of the adult metabolic syndrome: A systematic review. *Int. J. Obes.* **36**, 1–11 (2012).
8. F. Bacha, S. S. Gidding, Cardiac abnormalities in youth with obesity and type 2 diabetes. *Curr. Diab. Rep.* **16**, 62 (2016).
9. M. Simmonds, A. Llewellyn, C. G. Owen, N. Woolacott, Predicting adult obesity from childhood obesity: A systematic review and meta-analysis. *Obes. Rev.* **17**, 95–107 (2016).
10. J. J. Reilly, J. Kelly, Long-term impact of overweight and obesity in childhood and adolescence on morbidity and premature mortality in adulthood: Systematic review. *Int. J. Obes.* **35**, 891–898 (2011).
11. W. H. Dietz, M. C. Bellizzi, Introduction: The use of body mass index to assess obesity in children. *Am. J. Clin. Nutr.* **70**, 123S–125S (1999).
12. R. J. Kuczmarski et al., 2000 CDC Growth Charts for the United States: Methods and development. *Vital Health Stat. 11*, 1–190 (2002).
13. D. S. Freedman, B. Sherry, The validity of BMI as an indicator of body fatness and risk among children. *Pediatrics* **124** (suppl. 1), S23–S34 (2009).
14. A. Must, S. E. Anderson, Body mass index in children and adolescents: Considerations for population-based applications. *Int. J. Obes.* **30**, 590–594 (2006).
15. J. J. Reilly, Assessment of obesity in children and adolescents: Synthesis of recent systematic reviews and clinical guidelines. *J. Hum. Nutr. Diet.* **23**, 205–211 (2010).
16. D. S. Freedman et al., BMI z-Scores are a poor indicator of adiposity among 2- to 19-year-olds with very high BMIs, NHANES 1999-2000 to 2013-2014. *Obesity* **25**, 739–746 (2017).
17. World Health Organization, *Obesity: Preventing and Managing the Global Epidemic*, (World Health Organization, 2000).
18. National Institutes of Health, Clinical Guidelines on the Identification, Evaluation, and Treatment of Overweight and Obesity in Adults: The Evidence Report (National Heart, Lung, and Blood Institute, Bethesda, 1998), NIH Publication No. 98–4083. Available at https://www.nhlbi.nih.gov/health-pro/guidelines/archive/clinical-guidelines-obesity-adults-evidence-report. Accessed 1 March 2020.
19. P. Brambilla, G. Bedogni, M. Heo, A. Pietrobelli, Waist circumference-to-height ratio predicts adiposity better than body mass index in children and adolescents. *Int. J. Obes.* **37**, 943–946 (2013).
20. R. W. Taylor, I. E. Jones, S. M. Williams, A. Goulding, Evaluation of waist circumference, waist-to-hip ratio, and the conicity index as screening tools for high trunk fat mass, as measured by dual-energy X-ray absorptiometry, in children aged 3-19 y. *Am. J. Clin. Nutr.* **72**, 490–495 (2000).
21. C. Maffeis, A. Grezzani, A. Pietrobelli, S. Provera, L. Tatò, Does waist circumference predict fat gain in children? *Int. J. Obes. Relat. Metab. Disord.* **25**, 978–983 (2001).
22. S. Genovesi et al., Usefulness of waist circumference for the identification of childhood hypertension. *J. Hypertens.* **26**, 1563–1570 (2008).
23. S. C. Savva et al., Waist circumference and waist-to-height ratio are better predictors of cardiovascular disease risk factors in children than body mass index. *Int. J. Obes. Relat. Metab. Disord.* **24**, 1453–1458 (2000).
24. K. Karatzi et al.; Healthy Growth Study group, Cutoff points of waist circumference and trunk and visceral fat for identifying children with elevated inflammation markers and adipokines: The Healthy Growth Study. *Nutrition* **32**, 1063–1067 (2016).
25. H. D. McCarthy, Body fat measurements in children as predictors for the metabolic syndrome: Focus on waist circumference. *Proc. Nutr. Soc.* **65**, 385–392 (2006).
26. N. D. Volkow, G.-J. Wang, D. Tomasi, R. D. Baler, Obesity and addiction: Neurobiological overlaps. *Obes. Rev.* **14**, 2–18 (2013).
27. R. Pandit, J. W. de Jong, L. J. M. J. Vanderschuren, R. A. H. Adan, Neurobiology of overeating and obesity: The role of melanocortins and beyond. *Eur. J. Pharmacol.* **660**, 28–42 (2011).
28. H.-R. Berthoud, C. Morrison, The brain, appetite, and obesity. *Annu. Rev. Psychol.* **59**, 55–92 (2008).
29. N. S. Lawrence, E. C. Hinton, J. A. Parkinson, A. D. Lawrence, Nucleus accumbens response to food cues predicts subsequent snack consumption in women and increased body mass index in those with reduced self-control. *Neuroimage* **63**, 415–422 (2012).
30. K. E. Demos, T. F. Heatherton, W. M. Kelley, Individual differences in nucleus accumbens activity to food and sexual images predict weight gain and sexual behavior. *J. Neurosci.* **32**, 5549–5552 (2012).
31. R. B. Lopez, W. Hofmann, D. D. Wagner, W. M. Kelley, T. F. Heatherton, Neural predictors of giving in to temptation in daily life. *Psychol. Sci.* **25**, 1337–1344 (2014).
32. E. Green, A. Jacobson, L. Haase, C. Murphy, Reduced nucleus accumbens and caudate nucleus activation to a pleasant taste is associated with obesity in older adults. *Brain Res.* **1386**, 109–117 (2011).
33. K. M. Rapuano et al., Genetic risk for obesity predicts nucleus accumbens size and responsivity to real-world food cues. *Proc. Natl. Acad. Sci. U.S.A.* **114**, 160–165 (2017).
34. A. S. Bruce et al., Obese children show hyperactivation to food pictures in brain networks linked to motivation, reward and cognitive control. *Int. J. Obes.* **34**, 1494–1500 (2010).
35. B. J. Casey, A. Galván, L. H. Somerville, Beyond simple models of adolescence to an integrated circuit-based account: A commentary. *Dev. Cogn. Neurosci.* **17**, 128–130 (2016).
36. B. J. Casey, Beyond simple models of self-control to circuit-based accounts of adolescent behavior. *Annu. Rev. Psychol.* **66**, 295–319 (2015).
37. N. S. White et al., Improved conspicuity and delineation of high-grade primary and metastatic brain tumors using "restriction spectrum imaging": Quantitative comparison with high B-value DWI and ADC. *AJNR Am. J. Neuroradiol.* **34**, 958–964, S1 (2013).
38. N. S. White, T. B. Leergaard, H. D'Arceuil, J. G. Bjaalie, A. M. Dale, Probing tissue microstructure with restriction spectrum imaging: Histological and theoretical validation. *Hum. Brain Mapp.* **34**, 327–346 (2013).

NEUROSCIENCE

39. B. J. Casey et al.; ABCD Imaging Acquisition Workgroup, The Adolescent Brain Cognitive Development (ABCD) study: Imaging acquisition across 21 sites. Dev. Cogn. Neurosci. 32, 43–54 (2018).

40. G. J. Wang et al., Brain dopamine and obesity. Lancet 357, 354–357 (2001).

41. K. Blum et al., The D2 dopamine receptor gene as a determinant of reward deficiency syndrome. J. R. Soc. Med. 89, 396–400 (1996).

42. J. W. Cordeira, L. Frank, M. Sena-Esteves, E. N. Pothos, M. Rios, Brain-derived neurotrophic factor regulates hedonic feeding by acting on the mesolimbic dopamine system. J. Neurosci. 30, 2533–2541 (2010).

43. C. Hryhorczuk et al., Dampened mesolimbic dopamine function and signaling by saturated but not monounsaturated dietary lipids. Neuropsychopharmacology 41, 811–821 (2016).

44. N. D. Volkow et al., Brain dopamine is associated with eating behaviors in humans. Int. J. Eat. Disord. 33, 136–142 (2003).

45. T. E. Robinson, K. C. Berridge, The neural basis of drug craving: An incentive-sensitization theory of addiction. Brain Res. Brain Res. Rev. 18, 247–291 (1993).

46. K. C. Berridge, T. E. Robinson, Liking, wanting, and the incentive-sensitization theory of addiction. Am. Psychol. 71, 670–679 (2016).

47. K. C. Berridge, M. L. Kringelbach, Pleasure systems in the brain. Neuron 86, 646–664 (2015).

48. K. C. Berridge, T. E. Robinson, Parsing reward. Trends Neurosci. 26, 507–513 (2003).

49. B. G. Hoebel, Brain neurotransmitters in food and drug reward. Am. J. Clin. Nutr. 42, 1133–1150 (1985).

50. S. Fulton et al., Leptin regulation of the mesoaccumbens dopamine pathway. Neuron 51, 811–822 (2006).

51. I. S. Farooqi et al., Leptin regulates striatal regions and human eating behavior. Science 317, 1355 (2007).

52. D. M. Small, M. Jones-Gotman, A. Dagher, Feeding-induced dopamine release in dorsal striatum correlates with meal pleasantness ratings in healthy human volunteers. Neuroimage 19, 1709–1715 (2003).

53. W. K. Simmons et al., The ventral pallidum and orbitofrontal cortex support food pleasantness inferences. Brain Struct. Funct. 219, 473–483 (2014).

54. K. S. Smith, K. C. Berridge, The ventral pallidum and hedonic reward: Neurochemical maps of sucrose "liking" and food intake. J. Neurosci. 25, 8637–8649 (2005).

55. P. J. Morgane, Alterations in feeding and drinking behavior of rats with lesions in globi pallidi. Am. J. Physiol. 201, 420–428 (1961).

56. K. S. Smith, A. J. Tindell, J. W. Aldridge, K. C. Berridge, Ventral pallidum roles in reward and motivation. Behav. Brain Res. 196, 155–167 (2009).

57. C.-Y. Ho, K. C. Berridge, An orexin hotspot in ventral pallidum amplifies hedonic "liking" for sweetness. Neuropsychopharmacology 38, 1655–1664 (2013).

58. D. C. Castro, S. L. Cole, K. C. Berridge, Lateral hypothalamus, nucleus accumbens, and ventral pallidum roles in eating and hunger: Interactions between homeostatic and reward circuitry. Front. Syst. Neurosci. 9, 90 (2015).

59. A. J. Tindell, K. S. Smith, S. Peciña, K. C. Berridge, J. W. Aldridge, Ventral pallidum firing codes hedonic reward: When a bad taste turns good. J. Neurophysiol. 96, 2399–2409 (2006).

60. M. Valdearcos et al., Microglia dictate the impact of saturated fat consumption on hypothalamic inflammation and neuronal function. Cell Rep. 9, 2124–2138 (2014).

61. J. P. Thaler et al., Obesity is associated with hypothalamic injury in rodents and humans. J. Clin. Invest. 122, 153–162 (2012).

62. C. T. De Souza et al., Consumption of a fat-rich diet activates a proinflammatory response and induces insulin resistance in the hypothalamus. Endocrinology 146, 4192–4199 (2005).

63. X. Zhang et al., Hypothalamic IKKbeta/NF-kappaB and ER stress link overnutrition to energy imbalance and obesity. Cell 135, 61–73 (2008).

64. K. A. Posey et al., Hypothalamic proinflammatory lipid accumulation, inflammation, and insulin resistance in rats fed a high-fat diet. Am. J. Physiol. Endocrinol. Metab. 296, E1003–E1012 (2009).

65. H. Hsuchou et al., Obesity induces functional astrocytic leptin receptors in hypothalamus. Brain 132, 889–902 (2009).

66. J. G. Kim et al., Leptin signaling in astrocytes regulates hypothalamic neuronal circuits and feeding. Nat. Neurosci. 17, 908–910 (2014).

67. J. Molina et al., Reduced astrocytic expression of GFAP in the offspring of female rats that received hypercaloric diet. Nutr. Neurosci. 23, 411–421 (2020).

68. T. B. Ogassawara et al., Food deprivation in F0 generation and hypercaloric diet in F1 generation reduce F2 generation astrogliosis in several brain areas after immune challenge. Int. J. Dev. Neurosci. 64, 29–37 (2018).

69. L. Décarie-Spain et al., Nucleus accumbens inflammation mediates anxiodepressive behavior and compulsive sucrose seeking elicited by saturated dietary fat. Mol. Metab. 10, 1–13 (2018).

70. B. Pulli, J. W. Chen, Imaging neuroinflammation–From bench to bedside. J. Clin. Cell. Immunol. 5, 226 (2014).

71. D. S. Albrecht, C. Granziera, J. M. Hooker, M. L. Loggia, In vivo imaging of human neuroinflammation. ACS Chem. Neurosci. 7, 470–483 (2016).

72. A. H. Jacobs, B. Tavitian; INMiND consortium, Noninvasive molecular imaging of neuroinflammation. J. Cereb. Blood Flow Metab. 32, 1393–1415 (2012).

73. L. Capuron et al., Dopaminergic mechanisms of reduced basal ganglia responses to hedonic reward during interferon alfa administration. Arch. Gen. Psychiatry 69, 1044–1053 (2012).

74. L. Capuron et al., Basal ganglia hypermetabolism and symptoms of fatigue during interferon-alpha therapy. Neuropsychopharmacology 32, 2384–2392 (2007).

75. N. I. Eisenberger et al., Inflammation-induced anhedonia: Endotoxin reduces ventral striatum responses to reward. Biol. Psychiatry 68, 748–754 (2010).

76. L. P. Spear, The adolescent brain and age-related behavioral manifestations. Neurosci. Biobehav. Rev. 24, 417–463 (2000).

77. L. P. Spear, "Neurodevelopment during adolescence" in Neurodevelopmental Mechanisms in Psychopathology, D. Cicchetti, Ed. (Cambridge University Press, 2003), p. xii, pp. 62–83.

78. A. Galvan et al., Earlier development of the accumbens relative to orbitofrontal cortex might underlie risk-taking behavior in adolescents. J. Neurosci. 26, 6885–6892 (2006).

79. W. H. Dietz, Critical periods in childhood for the development of obesity. Am. J. Clin. Nutr. 59, 955–959 (1994).

80. J. N. Giedd, J. L. Rapoport, Structural MRI of pediatric brain development: What have we learned and where are we going? Neuron 67, 728–734 (2010).

81. J. Thompson et al., D2 dopamine receptor gene (DRD2) Taq1 A polymorphism: Reduced dopamine D2 receptor binding in the human striatum associated with the A1 allele. Pharmacogenetics 7, 479–484 (1997).

82. K. S. Burger, E. Stice, Variability in reward responsivity and obesity: Evidence from brain imaging studies. Curr. Drug Abuse Rev. 4, 182–189 (2011).

83. E. Stice, K. Burger, Neural vulnerability factors for obesity. Clin. Psychol. Rev. 68, 38–53 (2019).

84. E. Stice, S. Spoor, C. Bohon, D. M. Small, Relation between obesity and blunted striatal response to food is moderated by TaqIA A1 allele. Science 322, 449–452 (2008).

85. P. Srikanthan, T. E. Seeman, A. S. Karlamangla, Waist-hip-ratio as a predictor of all-cause mortality in high-functioning older adults. Ann. Epidemiol. 19, 724–731 (2009).

86. W. A. Marshall, J. M. Tanner, Variations in pattern of pubertal changes in girls. Arch. Dis. Child. 44, 291–303 (1969).

87. W. A. Marshall, J. M. Tanner, Variations in the pattern of pubertal changes in boys. Arch. Dis. Child. 45, 13–23 (1970).

88. J.-C. Desmangles, J. M. Lappe, G. Lipaczewski, G. Haynatzki, Accuracy of pubertal Tanner staging self-reporting. J. Pediatr. Endocrinol. Metab. 19, 213–221 (2006).

89. J. Brooks-Gunn, M. P. Warren, J. Rosso, J. Gargiulo, Validity of self-report measures of girls' pubertal status. Child Dev. 58, 829–841 (1987).

90. K. Lee, B. Valeria, C. Kochman, C. M. Lenders, Self-assessment of height, weight, and sexual maturation: Validity in overweight children and adolescents. J. Adolesc. Health 39, 346–352 (2006).

91. S. Bonat, A. Pathomvanich, M. F. Keil, A. E. Field, J. A. Yanovski, Self-assessment of pubertal stage in overweight children. Pediatrics 110, 743–747 (2002).

92. S. E. Anderson, G. E. Dallal, A. Must, Relative weight and race influence average age at menarche: Results from two nationally representative surveys of US girls studied 25 years apart. Pediatrics 111, 844–850 (2003).

93. P. B. Kaplowitz, Link between body fat and the timing of puberty. Pediatrics 121 (suppl. 3), S208–S217 (2008).

94. M. I. Goran, B. A. Gower, Longitudinal study on pubertal insulin resistance. Diabetes 50, 2444–2450 (2001).

95. A. Kleinridders et al., Insulin resistance in brain alters dopamine turnover and causes behavioral disorders. Proc. Natl. Acad. Sci. U.S.A. 112, 3463–3468 (2015).

96. C. B. Jasik, R. H. Lustig, Adolescent obesity and puberty: The "perfect storm". Ann. N. Y. Acad. Sci. 1135, 265–279 (2008).

97. G. Fantuzzi, R. Faggioni, Leptin in the regulation of immunity, inflammation, and hematopoiesis. J. Leukoc. Biol. 68, 437–446 (2000).

98. A. Aguilar-Valles, W. Inoue, C. Rummel, G. N. Luheshi, Obesity, adipokines and neuroinflammation. Neuropharmacology 96, 124–134 (2015).

99. X. Wang, V. A. Villar, A. Tiu, K. K. Upadhyay, S. Cuevas, Dopamine D2 receptor upregulates leptin and IL-6 in adipocytes. J. Lipid Res. 59, 607–614 (2018).

100. D. C. Borcherding et al., Dopamine receptors in human adipocytes: Expression and functions. PLoS One 6, e25537 (2011).

101. W. M. Compton, G. J. Dowling, H. Garavan, Ensuring the best use of data: The adolescent brain cognitive development study. JAMA Pediatr., 10.1001/jamapediatrics.2019.2081 (2019).

102. T. L. Jernigan, S. A. Brown; ABCD Consortium Coordinators, Introduction. Dev. Cogn. Neurosci. 32, 1–3 (2018).

103. R. A. Carper, J. M. Treiber, N. S. White, J. S. Kohli, R.-A. Müller, Restriction spectrum imaging as a potential measure of cortical neurite density in autism. Front. Neurosci. 10, 610 (2017).

104. H. Garavan et al., Recruiting the ABCD sample: Design considerations and procedures. Dev. Cogn. Neurosci. 32, 16–22 (2018).

105. M. A. Carskadon, C. Acebo, A self-administered rating scale for pubertal development. J. Adolesc. Health 14, 190–195 (1993).

106. R. Q. Loi et al., Restriction spectrum imaging reveals decreased neurite density in patients with temporal lobe epilepsy. Epilepsia 57, 1897–1906 (2016).

107. D. J. Hagler et al., Image processing and analysis methods for the Adolescent Brain Cognitive Development Study. Neuroimage 202, 116091 (2019).

108. R Core Team, R: A Language and Environment for Statistical Computing (R Foundation for Statistical Computing, Vienna, 2013). https://www.r-project.org/.

109. D. Bates, M. Mächler, B. Bolker, S. Walker, Fitting linear mixed-effects models using lme4. J. Stat. Softw. 67, 1–48 (2015).

110. Centers for Disease Control and Prevention, A SAS Program for the 2000 CDC Growth Charts (Ages 0 to <20 years) (2016) https://www.cdc.gov/nccdphp/dnpao/growthcharts/resources/sas.htm. (Accessed 1 September 2018).